1   Supporting information

2

3   **SO$_2$ initiates the efficient conversion of NO$_2$ to HONO on MgO surface**

4   Qingxin Ma[1,2*], Tao Wang[1*], Chang Liu[3], Hong He[2], Zhe Wang[1], Weihao Wang[1], Yutong Liang[1]

5

6   *1. Department of Civil and Environmental Engineering, The Hong Kong Polytechnic*
7   *University, Kowloon, Hong Kong, 999077, China*

8   *2. Research Center for Eco-Environmental Sciences, Chinese Academy of Sciences,*
9   *Beijing 100085, China*

10   *3. State Key Laboratory of Severe Weather & Key Laboratory of Atmospheric*
11   *Chemistry of China Meteorological Administration, Chinese Academy of*
12   *Meteorological Sciences, Beijing 100081, China*

13

14   Corresponding author.

15   E-mail address: cetwang@polyu.edu.hk (T. Wang); qxma@rcees.ac.cn (Q.X. Ma).
16   Tel.: +86 852 27666059; fax: +86 852 23346389.

17

18   The supporting information has 10 pages including 9 figures.

19

20

21

22

23

24

25

26   The uptake experiments were performed in a horizontal cylindrical coated-wall
27   flow tube reactor (34 cm length, 1.6 cm i.d.). Figure S1 shows the diagram of the flow
28   tube reactor. The powder samples were coated onto a quartz tube (20.0 cm length, 1.1
29   cm i.d., and 1.5 cm o.d.). An O-ring was used to make the air tight between the inner
30   wall of reactor tube and the outer wall of sample tube. The experiments were
31   performed at ambient pressure and maintained at 295 K by circulating water bath
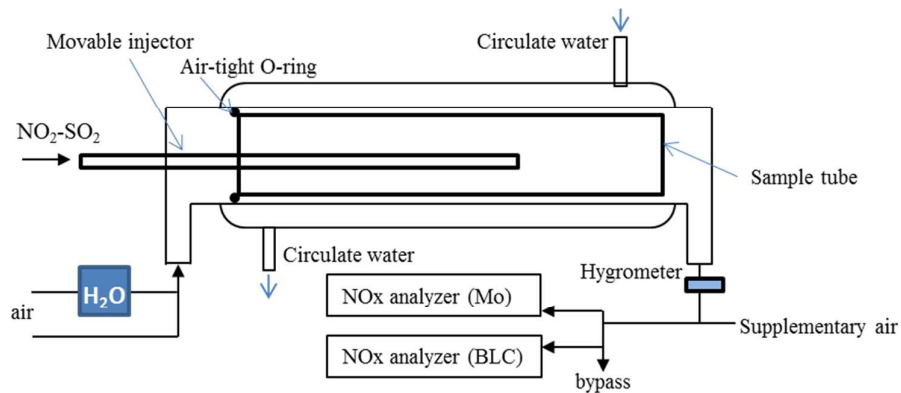32   through the outer jacket of the flow tube reactor.

33

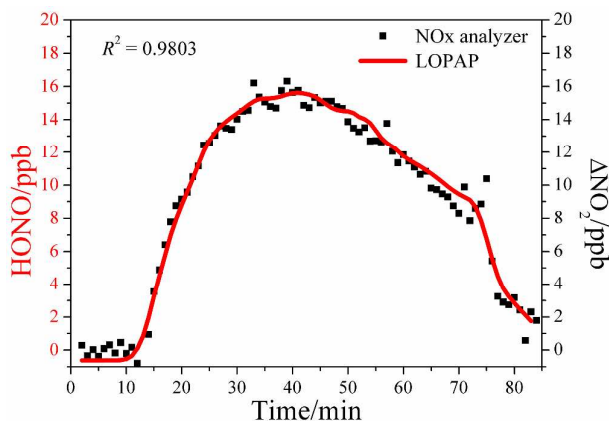34   Figure S1. Diagram of the flow tube

35

Figure S2. Comparison of the measurement results between LOPAP (red line) and difference of two NOx-analyzers (black square).

HONO formed in the uptake of NO_2 on SO_2-aged MgO was measured simultaneously with two NOx analyzers (THERMO 42i) and a long path absorption photometer (QUMA, Model LOPAP-03). A brief description of this instrument is provided as follows. Further details can be found in Heland et al.[1] and Xu et al.[2] The gas flow was sampled in two similar temperature controlled stripping coils in series using a mixture reagent of 100 g sulfanilamide and 1 L HCl (37% volume fraction) (R1) in 9 L pure water. In the first stripping coil, almost all of the HONO and a fraction of interfering substances were absorbed in solution. In the second stripping coil, about the same amount of the interfering species but almost no HONO were absorbed in solution. After adding a reagent of 1.6 g N-naphtylethylendiamine-dihydrochloride (R2) in 9 L pure water to both coils, colored azo dye was formed in the solution of R1 and R2, which were then separately detected via long path absorption in special Teflon tubing. The interference free HONO signal was the difference between the signals in the two channels. The calibration of the channels is performed with a liquid nitrite standard, which is injected into R1 at known amounts (corresponding to 5 ppbv and 10 ppbv HONO).

A good correlation (R^2=0.9803) was found between LOPAP result and the difference of two NOx analyzers. Therefore, in the main text, the ΔNO_2 measured from two NOx analyzers was referred to HONO.
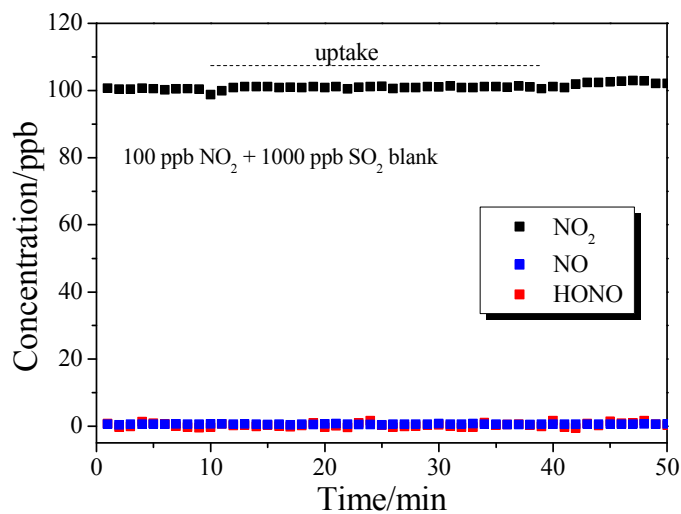
Figure S3. Uptake of 100 ppb NO_2 on the blank tube in the presence of 1000 ppb SO_2.
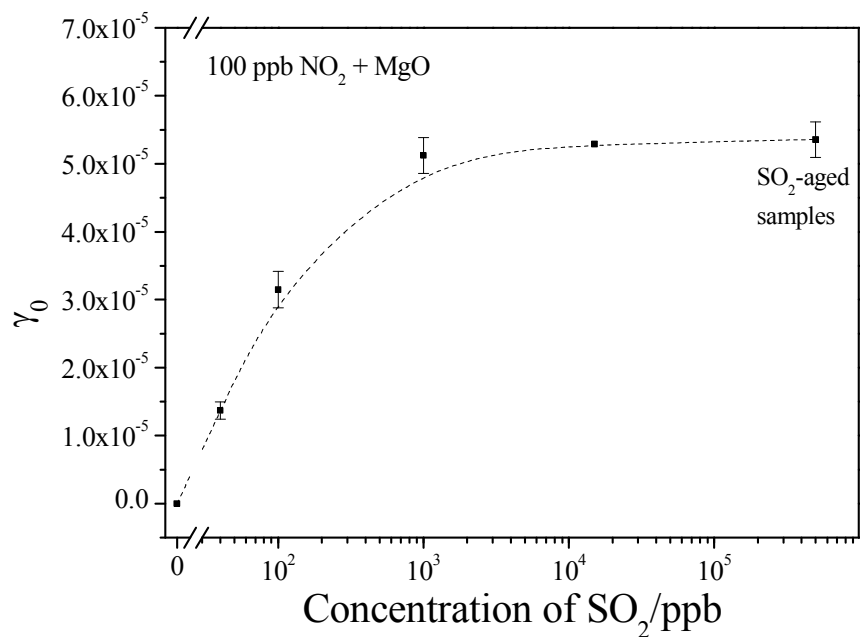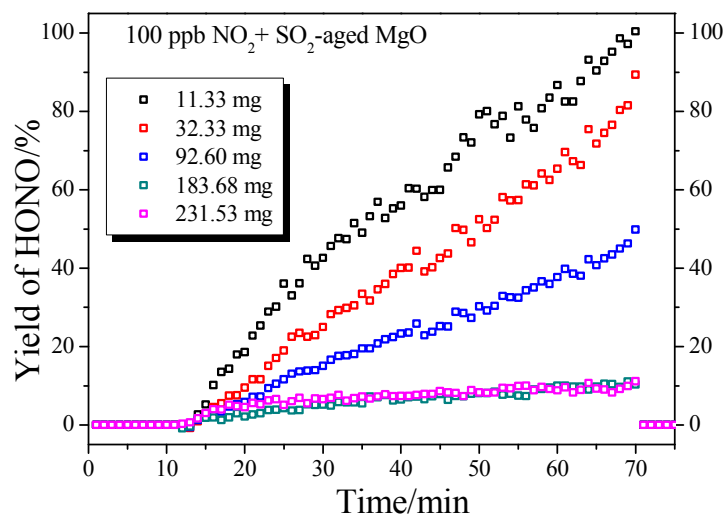RH=7.5%.

Figure S4. Effect of SO_2 concentration on the uptake coefficients (γ_0) of NO_2 on MgO at 7.5%
RH. The dash line is drawn to guide the eye.
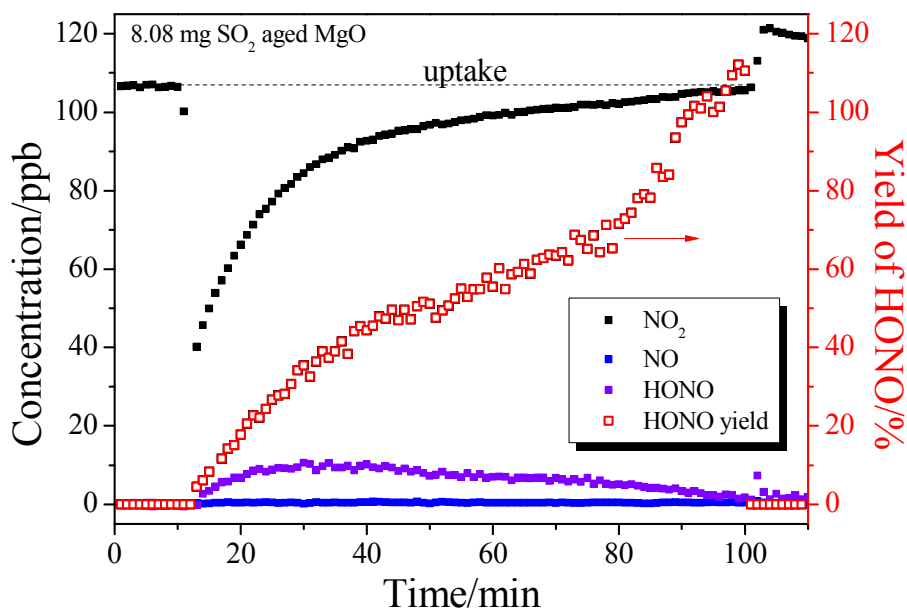
70

Figure S5. The measured yields of HONO on different weight of samples during the uptake of
100 ppb NO_2 on SO_2-aged MgO at 7.5% RH.

Figure S6. Uptake of NO_2 and the measured yields of HONO on 8.08 mg SO_2-aged MgO at
7.5% RH.

81

The chart shows y-axis labeled "K-M" ranging from 0.000 to 0.040, and x-axis labeled "Wavenumber/cm^{-1}" ranging from 2000 to 800. The plot title reads "200 ppb NO$_2$ + MgO" with spectra labeled 180 min, 120 min, 60 min, 30 min, 10 min, and 0 min.

82
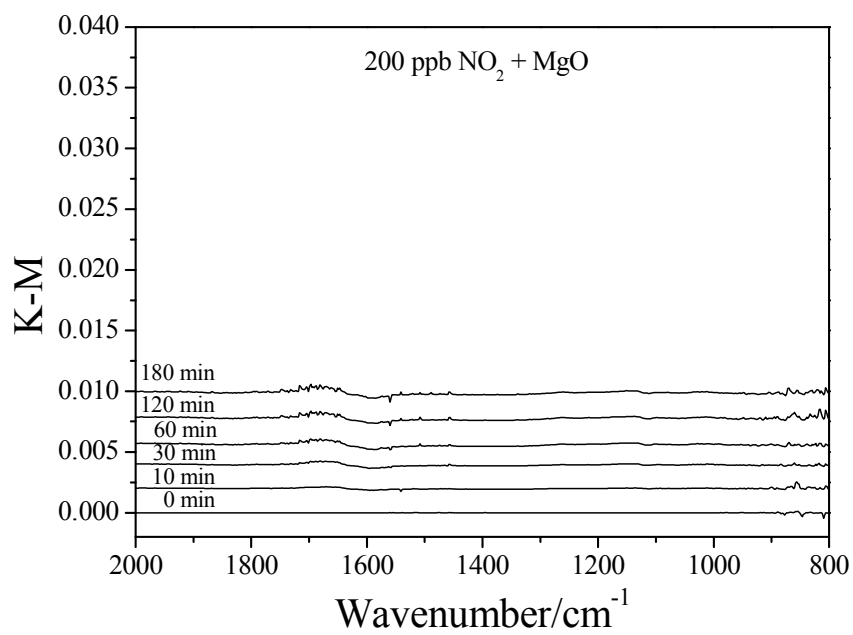
Figure S7. *In situ* DRIFTS spectra of MgO exposed to 200 ppb NO$_2$ as a function of time.

84

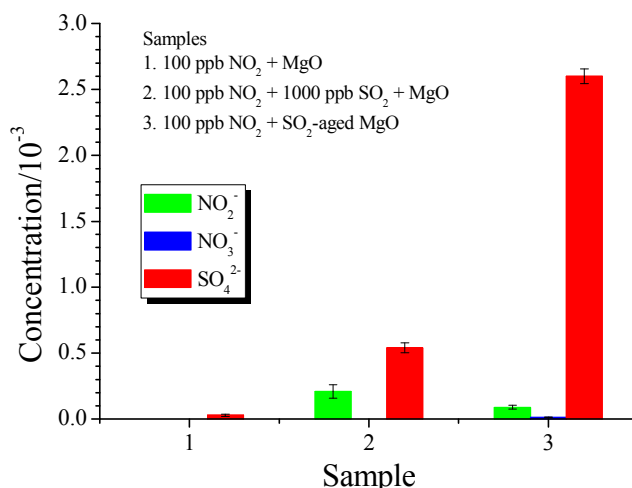Figure S8. Comparison of the concentrations of water soluble ions on surface by IC.

Water-soluble inorganic anions were analyzed using an ion chromatograph (ICS-1000, Dionex Corporation) which consists of a guard column (AG14A) and an analytical column (AS14A). An electrolytic suppressor (ASRS 300 4-mm) was used to reduce the conductivity of the eluent. A concentrator (TAC-LP1) was installed. The analysis was performed by using 8 mM sodium carbonate/ 1 mM sodium bicarbonate eluent at a flow rate of 0.6 mL min^{-1}. Multi-point calibrations were performed by using calibration standard solutions (Dionex Corporation, seven anion standards for anion). Good linearity of the calibration curve was obtained with $R^2 > 0.996$. The anions NO_2^-, NO_3^- and SO_4^{2-}, were analyzed. SO_3^{2-} was not analyzed because the column is not able to analyze SO_3^{2-} ion.

The samples were prepared under the same conditions as uptake experiments stated in the main text, and then were extracted using deionized water. None nitrite and nitrate was observed in the reaction between 100 ppb NO_2 and MgO, indicating low reactivity of MgO to NO_2 with low concentration. This was in consistent with the results of flow tube and DRIFTS experiments. The sulfate observed in this reaction was due to the residual impurity of sulfate in MgO agent (<100 mg/kg). Nitrite and sulfate were produced in the reaction between NO_2 & SO_2 and MgO. None nitrate was observed because the excess SO_2 could reduce the NO_2 to nitrite completely. Large amount of sulfate was observed in the reaction between 100 ppb NO_2 and SO_2-aged MgO. This was due to the formation of surface sulfate during the ageing process. Nitrite was produced by the reaction between NO_2 and surface sulfite species. A minute quantity of nitrate was also observed in this reaction, which might be due to the reaction of NO_2 with H_2O on MgO surface.
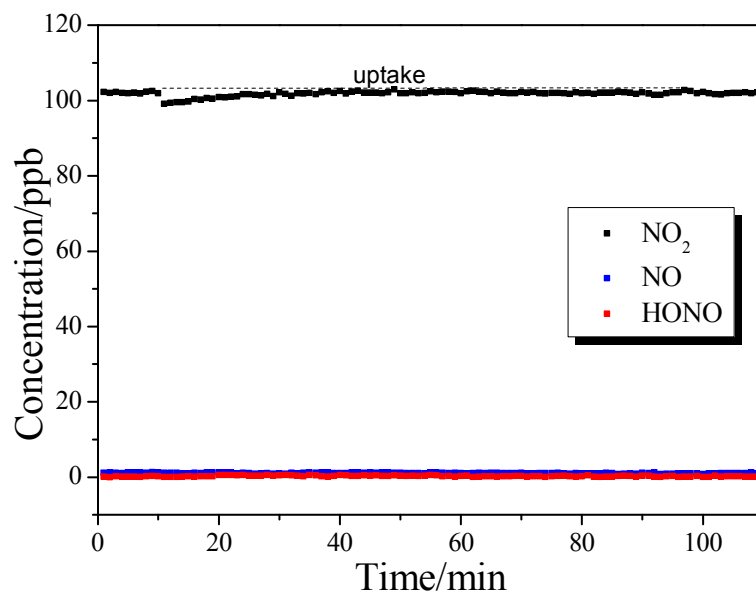
113

114   Figure S9. Uptake of 100 ppb NO_2 on SO_2+O_3 aged MgO (26.38 mg). RH=7.5%. The ageing

115   process: MgO was first exposed to 1000 ppb SO_2 for 12 h and then exposed to 500 ppb O_3 for

116   2 h in synthetic air. The aim of the aging process was to force oxdize surface sulfite to sulfate.

117

118   Calculation of HONO formation rate

119   The NO_2 conversion was calculated using the following equation:[3]

$$\frac{\%NO_2}{h} = \frac{1}{4} \times v_{NO_2} \times S/V \times \gamma \times 3600 \times 100$$

120   where, v_{NO2} is the mean molecular velocity of NO_2 (m s^{-1}), S/V is the aerosol surface
121   to volume ratio (m^{-1}) representing the surfaces available for heterogeneous reaction,
122   and γ is the uptake coefficient of NO_2 at the aerosol surface.

123   As shown in the main text, the yield of HONO and nitrite in the uptake of NO_2 was
124   about 100%. Then the formation rate of HONO is equal to that of NO_2 conversion
125   rate.

126   For the ground surface, the S/V was adopted a constant value of 0.3 m^{-1}.[4, 5] The
127   proportion of MgO (1.7%) in the soil in the north China plain was based on the
128   analysis of Fang et al.[6]

129   As for aerosol, the mass concentration of $PM_{2.5}$ was basen on the field measurement
130   of Hou et al.[7], and the average ratio of $PM_{2.5}/PM_{10}$ (0.5) during haze-fog episodes in
131   Beijing was used to estimate the mass concentration of PM_{10}.[8] The relation between
132   mass concentration and surface area of aerosol in Beijing was based on the values
133   measured in Wu et al., in which ~10^{-5} m^2 µg^{-1} of particles was determined[9].

134

135

136

137

138   Reference

139   1.   Heland, J.; Kleffmann, J.; Kurtenbach, R.; Wiesen, P., A new instrument to measure
140   gaseous nitrous acid (HONO) in the atmosphere. *Environ. Sci. Technol.* **2001,** *35*, (15),
141   3207-3212.
142   2.   Xu, Z.; Wang, T.; Wu, J.; Xue, L.; Chan, J.; Zha, Q.; Zhou, S.; Louie, P. K.; Luk, C. W.,
143   Nitrous acid (HONO) in a polluted subtropical atmosphere: Seasonal variability, direct vehicle
144   emissions and heterogeneous production at ground surface. *Atmos. Environ.* **2015,** *106*,
145   100-109.
146   3.   Kleffmann, J.; Becker, K.; Wiesen, P., Heterogeneous NO_2 conversion processes on acid
147   surfaces: possible atmospheric implications. *Atmos. Environ.* **1998,** *32*, (16), 2721-2729.
148   4.   Sarwar, G.; Roselle, S. J.; Mathur, R.; Appel, W.; Dennis, R. L.; Vogel, B., A comparison of
149   CMAQ HONO predictions with observations from the Northeast Oxidant and Particle Study.
150   *Atmos. Environ.* **2008,** *42*, (23), 5760-5770.
151   5.   Zhang, L.; Wang, T.; Zhang, Q.; Zheng, J.; Xu, Z.; Lv, M., Potential Sources of Nitrous Acid
152   (HONO) and Their Impacts on Ozone: A WRF‐Chem study in a Polluted Subtropical Region.
153   *J. Geophys. Res.* **2016**.
154   6.   Fang, W.; Peng, L.; Gendi, X., Review of magnesium in soil and its effectiveness. *Journal*
155   *of Henan Agricultural sciences* **2004,** *33*, (1), 22-36. (in Chinese)
156   7.   Hou, S.; Tong, S.; Ge, M.; An, J., Comparison of atmospheric nitrous acid during severe
157   haze and clean periods in Beijing, China. *Atmos. Environ.* **2016,** *124*, 199-206.
158   8.   Sun, Y.; Zhuang, G.; Tang, A.; Wang, Y.; An, Z., Chemical characteristics of $PM_{2.5}$ and
159   PM10 in haze-fog episodes in Beijing. *Environ. Sci. Technol.* **2006,** *40*, (10), 3148-3155.
160   9.   Wu, Z.; Hu, M.; Lin, P.; Liu, S.; Wehner, B.; Wiedensohler, A., Particle number size
161   distribution in the urban atmosphere of Beijing, China. *Atmos. Environ.* **2008,** *42*, (34),
162   7967-7980.

163